

Experimental and Theoretical Study of the Transannular Intramolecular Interaction and Cage Effect in the Atrane Framework of Boratrane and 1-Methylsilatrane

Alexander A. Korlyukov,^{*,†} Konstantin A. Lyssenko,[†] Mikhail Yu. Antipin,^{*,†} Valerii N. Kirin,[‡] Eugenio A. Chernyshev,[†] and Sergei P. Knyazev[†]

A. N. Nesmeyanov Institute of Organoelement Compounds (INEOS) of the Russian Academy of Sciences, 28 Vavilov St., B-334, 119991 Moscow, Russian Federation, and Moscow State Academy of Fine Chemical Technology, 117571 Moscow, Russian Federation

Received August 6, 2001

On the basis of the high-resolution single-crystal X-ray diffraction data and theoretical B3LYP/6-311+G(d) and B3LYP/cc-pVDZ calculations, the electron density distribution in boratrane and 1-methylsilatrane has been investigated. The B–N bond in the boratrane molecule was found to correspond to the “shared” (covalent) interatomic interaction in terms of Bader’s “atoms in molecules” (AIM) theory. On the contrary, the Si···N bond in 1-methylsilatrane and B–N bond in a series of some acyclic donor–acceptor boron complexes and other boratrane derivatives correspond to interaction of an “intermediate” type. Such character of the B–N bond is caused by an influence of the atrane “cage effect”. The influence of this effect results in deformation of the boron atom and displacement of the bond critical point (3,–1) to the region of the electron lone pair of the nitrogen atom. This changes the type of the interatomic interaction in comparison to other compounds investigated and explains high hydrolytic stability of boratrane as well as silatranes and germatranes.

Introduction

Atranes and related tricyclic compounds (Figure 1) represent organoelement “hypervalent” molecules, which are characterized by thermodynamic stability and resistance to hydrolysis. Many of their properties are explained as a result of the M···N intramolecular interaction which leads to expansion of the coordination sphere of the central atom M.

Silicon atranes (silatranes) are the most known and widely investigated compounds in the mentioned series. A general structural feature of atranes is dependence of the M···N distance on the inductive effect of the substituent X. This dependence was used to prove several theoretical concepts describing the nature of the M···N interaction either as a transfer of the nitrogen electron lone pair (Lp) to vacant 3d orbitals of the Si atom^{1,2} or as a dative bond transfer of the

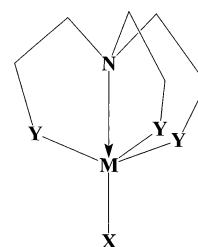


Figure 1. Atranes for which M = Si, B, Ge, and Sn, Y = O, N, C, and S, and X = Alk, Ar, and Hal.

nitrogen Lp to the lowest unoccupied orbital of the M···N bond.³ The usefulness of the latter model for atranes was recently confirmed by theoretical investigations.³

In addition to a substituent inductive effect, the Si···N distance in silatranes depends also on the nature of the equatorial atom Y. Replacement of oxygen atoms by nitrogen and carbon ones³ results in rather small variation in the Si···N distances, while atranes with only partially replaced

* To whom correspondence should be addressed. E-mail: alex@xrlab.ineos.ac.ru (A.A.K.); mishan@xray.ineos.ac.ru (M.Y.A.). Fax: +7 095 135 5085 (A.A.K., M.Y.A.).

[†] A. N. Nesmeyanov Institute of Organoelement Compounds (INEOS) of the Russian Academy of Sciences.

[‡] Moscow State Academy of Fine Chemical Technology.

(1) Voronkov, M. G.; Baryshok, V. P. *J. Organomet. Chem.* **1982**, *239*, 199–249.

(2) Hencel, P.; Parkanyi, L. *The molecular structure of silatranes*; Reviews on silicon, germanium, tin and lead compounds; Gielen, M., Ed.; Freund Publ. House: Tel-Aviv, 1985.

(3) Schmidt, M. W.; Windus, T. L.; Gordon, M. S. *J. Am. Chem. Soc.* **1995**, *117*, 7480–7486.

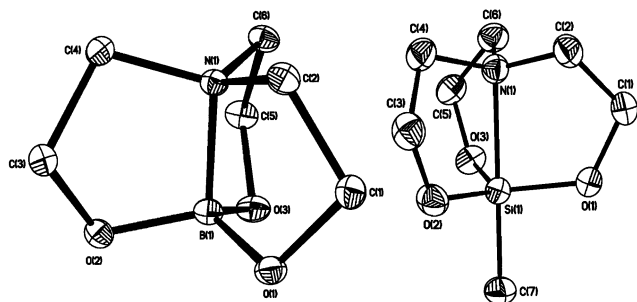


Figure 2. General view of the molecules **1** and **2** in their crystals. Atoms are presented by thermal ellipsoids drawn at 80% probability.

equatorial oxygens are characterized by conformational distortions. These distortions give rise to significant weakening of the Si \cdots N interaction.^{1,2}

One may suppose that high hydrolytic resistance of silatranes is caused by several factors. The first one is the presence of the atrane cage which causes shielding of the central atom M from attack of a reagent (i.e. water). The second factor is strong decrease of the basic power of the nitrogen atom Lp's because of its coordination with the central atom M. These factors act cooperatively and cannot be distinguished; further they will be referred to as an atrane "cage effect". Existing models of the Si \cdots N transannular interaction cannot, however, explain this effect. Therefore, it is interesting to investigate some atranes, where the nature of the M \cdots N intramolecular interaction is well-known, and the boratrane molecule seems to be the most suitable example for such an investigation. The intramolecular B–N interaction in boratrane represents a typical donor–acceptor bond which is realized in many donor–acceptor boron complexes.⁴

To analyze the nature of bonding in atranes, in the present work the electron density distribution in boratrane (**1**) and 1-methylsilatrane (**2**) was studied⁵ (Figure 2) on the basis of high-resolution single-crystal X-ray diffraction data at 100 K and theoretical DFT calculations.

To investigate the atrane cage effect, acyclic boron compound B(NH₂)₃ (**3**), where the B–N bond is formed by means of an exchanging mechanism, and BH₃NH₃ (**4**), in which the B–N bond has dative character, have been studied as well using theoretical calculations. Finally, to evaluate the effect of equatorial atoms the acyclic compound (HO)₃BNH₃ (**5**) and a series of boratrane derivatives in which equatorial oxygen atoms are replaced by nitrogen (**6**), sulfur (**7**), and carbon (**8**) atoms were studied as well (Figure 3).

Chemical bonding in the compounds studied was investigated using topological analysis of the electron density distribution (EDD) function $\rho(r)$ in terms of Bader's "atoms in molecules" theory (AIM).⁶ This approach is based on analysis values of the total electron density $\rho(r)$, its Laplacian

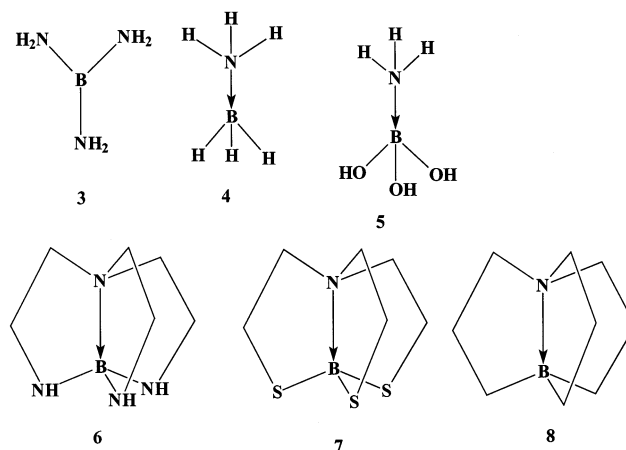


Figure 3. Chemical formulas of the calculated model compounds.

$\nabla^2\rho(r)$, and contributions of the local kinetic and potential energy densities to the total local electron energy $E(r)$ in the bond critical points (CP) where the gradient of the $\rho(r)$ vanishes. Usually, the main attention in the AIM theory is paid to CP(3,–1), i.e., "saddle" points in the relief of the $\rho(r)$, and the presence of this CP is a universal indicator of chemical bond. According to the AIM, interatomic interactions fall into "shared" and "closed-shell" types. Shared (covalent) interactions are characterized by the negative $\nabla^2\rho(r)$ values and high $\rho(r)$ values in CP(3,–1), while in the case of closed-shell interactions (ionic bonds, some van der Waal complexes, etc.) the value of the $\nabla^2\rho(r)$ is positive and the total $\rho(r)$ in CP(3,–1) is small. However, a positive $\nabla^2\rho(r)$ value is not a unique criteria of the closed-shell interaction. The necessary condition for realization of this type of interaction is a positive value of the local energy density which is related to $\nabla^2\rho(r)$ by the equation $E(r) = V(r) + G(r) = G(r) - (\hbar^2/4m) \nabla^2\rho(r)$,⁶ where $V(r)$ and $G(r)$ are the local potential and kinetic energy densities, respectively. It can be seen from this equation that if the $\nabla^2\rho(r)$ is positive, the value of the $E(r)$ may remain still negative if the potential energy density (a priori negative) exceeds the kinetic one in absolute value. Therefore, the bonds which are characterized by a positive value of the $\nabla^2\rho(r)$ and negative value of the $E(r)$ are often referred to as an "intermediate type" of interatomic interaction (some H-bonds, donor–acceptor bonds, etc.). We may note that this empirical classification of chemical bonds as an exhibition of different types of interatomic interactions is based mostly on the relation between signs of the Laplacian of the electron density and local energy density values in the corresponding CP's.

The AIM theory is successfully used nowadays for the description of different chemical bonds and interatomic interactions including as well unusual intra- and intermolecular contacts, hydrogen bonds, chemical bonding in hypervalent and electron deficient polyhedral compounds,^{7–9} etc., in terms of observable characteristics of the $\rho(r)$.

(4) Boese, R.; Niederprum, N.; Blaser, D. *Molecules in natural science and medicine*; 1991; p 103.

(5) Crystal structures of **1** and **2** have been investigated previously at ambient temperature: (a) Wu-Jiang, L.; Man-Shui, H.; Ming-Sheng, H.; Sheng-Zhi, H. *Chin. J. Struct. Chem. (Jiegou Huaxue)* **1991**, *10*, 258. (b) Matters, R.; Fenske, D.; Tebbe, K. F. *Chem. Ber.* **1972**, *105*, 2089.

(6) Bader, R. F. W. *Atoms in molecules. A quantum theory*; Clarendon Press: Oxford, U.K., 1990.

(7) Antipin, M. Y.; Boese, R.; Blaser, D.; Maulitz, A. *J. Am. Chem. Soc.* **1997**, *119*, 326–333.

(8) Lyssenko, K. A.; Antipin, M. Y.; Lebedev, V. N. *Inorg. Chem.* **1998**, *37*, 5834–5843.

(9) Espinosa, E.; Mollins, E.; Lecomte, C. *Chem. Phys. Lett.* **1998**, *285*, 170.

Previous MP2/TZ2P theoretical analysis¹⁰ of the EDD in a series of some boron donor–acceptor complexes has demonstrated that the dative B–N bond is characterized by a positive value of the $\nabla^2\rho(r)$ in the CP(3, –1) and a negative value of the $E(r)$ in contrast to usual covalent polar bonds ($\nabla^2\rho(r) < 0$, $E(r) < 0$) formed by pairing electrons from both participating atoms. Therefore, according to mentioned classification of atomic interactions, this bond was considered as an interaction of intermediate type. Positive value of $\nabla^2\rho(r)$ was found also in the CP(3, –1) for the Si \cdots N interaction in 1-methylsilatrane (data were obtained with MP2/6-31G(d) calculations and from an experimental EDD study^{11,12}). Despite that evaluation of $E(r)$ was not carried out,^{10–12} the absolute values of $\rho(r)$ and $\nabla^2\rho(r)$ in the CP's(3, –1) for both B–N and Si–N bonds allowed one to make a preliminary conclusion that both these bonds correspond to the intermediate type of interatomic interaction.

Results and Discussion

Molecular Geometry. The molecular geometries of compounds with dative bonds demonstrate pronounced features which distinguish them from ordinary covalent bonds.¹³ It was pointed out by the gas electron diffraction (ED) analysis of 1-methylsilatrane and BH₃NH₃^{14,15} that dative bonds in these compounds are considerably elongated in the gas phase in comparison to the solid state (up to 0.3 Å for 1-methylsilatrane). In the literature such compounds often referred to as “partially bonded molecules”.¹⁶

The B3LYP-calculated B \cdots N distance in BH₃NH₃ (1.654 and 1.662 Å for 6-311+G(d) and cc-pVDZ basis sets, respectively) is significantly longer than that in the crystal (1.564(6) Å),⁴ but it is close to the experimental value in the gas phase as well as to values obtained in CI, MP2, and MP4 calculations.^{10,17,18}

Similarly, the B \cdots N distance in boratrane is considerably elongated in the gas phase. Recent ED data have shown that the B–N bond in this compound is equal to 1.84(4) Å¹⁹ in comparison to 1.6764(3) Å in the crystal state at 100 K (Table 1). The theoretically calculated B–N bond length is equal to 1.8283 and 1.8384 Å for B3LYP/cc-pVDZ and B3LYP/6-311+G(d) calculations, which is close to the ED data.²⁰ Thus, selected method/basis combinations (B3LYP/

Table 1. Important Bond Lengths (Å) in the Compounds Studied

compound	bond	method of investigation		
		B3LYP/6-311+G(d)	B3LYP/cc-pVDZ	X-ray/gas phase
1	B–N	1.838	1.828	1.6764(7)/1.84(4)
	B–O	1.429	1.450	1.4450
2	Si \cdots N	2.672	2.561	2.1604(3)/2.45(6)
	Si–O	1.673	1.703	1.6791
3	B–N	1.433	1.432	1.438
4	B–N	1.654	1.662	1.564(6)/1.657
	B–O	1.432	1.432	
5	B–N	1.759	1.759	
	B–O	1.432	1.432	
6	B–N	1.696	1.699	
	B–N	1.531	1.532	
7	B–N	1.718	1.729	
	B–S	1.913	1.913	
8	B–N		1.758	
	B–C		1.632	

6-311+G(d) and B3LYP/cc-pVDZ) seem to be reliable enough for the B–N bond description.

The Si \cdots N distance in 1-methylsilatrane obtained by B3LYP/cc-pVDZ (2.561 Å) is also comparable to the experimental data in the gas phase, and it also elongated in comparison to the crystal state (2.1604(3) Å). Results of the B3LYP/6-311+G(d) calculation give rise to unreasonable Si \cdots N distance elongation (2.672 Å) that allowed one to disregard the data obtained by this method/basis for this molecule.

The B–N bond in B(NH₂)₃ (1.433 and 1.432 Å for B3LYP/6-311+G(d) and B3LYP/cc-pVDZ calculations) is close to that for the analogous bond in HB(NH₂)₃ calculated by MP2/DZP (1.424 Å).²⁰ The transition from the isolated molecule to the crystal does not change significantly the B–N bond length in these compounds, which is supported by available experimental X-ray data for B(NMe₂)₃ (1.437 Å).²¹ All other bonds in the atrane framework in the boratrane and 1-methylsilatrane are not changed significantly when going from the gas phase to the crystal state.

On the basis of the the molecular geometry only, one may suggest that the B–N bond in boratrane is considerably weaker than that in BH₃NH₃, and the nature of this bond may be similar to the Si \cdots N dative bond in 1-methylsilatrane.

Let us analyze structural changes occurring during the transition of atranes from the gas phase to the crystal. To do it, analysis of the atrane structures taken from the Cambridge Structural Database²² was made. Only ordered structures with M = Si and Ge, X = Hal, Alk, and OAlk, and *R*-values below 0.1 were taken into consideration. The retrieved data revealed that in most of the atranes deviation of the nitrogen atom from the plane of the carbons (*D_N*) varies in a rather narrow interval (0.33–0.42 Å). This may indicate that donation capacity of the nitrogen Lp does not change very much. The boratrane and 1-methylsilatrane also have a pyramidal configuration of the nitrogen atoms both in the crystalline phase (*D_N* values are equal to 0.35 and 0.37 Å) and in the isolated molecules (0.29 and 0.25 Å). It was found also that in the boratrane derivatives **6–8** the *D_N* values (0.34–0.38 Å) are almost the same as in the crystal due to shorter B–N bonds in comparison with boratrane. The only

(10) Jonas, V.; Frenking, G.; Reetz, M. T. *J. Am. Chem. Soc.* **1994**, *116*, 8741–8753.

(11) Anglada, J. P.; Bo, C.; Bofill, J. M.; Crehuet, R.; Poblet, J. M. *Organometallics* **1999**, *8*, 5584–5593.

(12) Lyssenko, K. A.; Korlyukov, A. A.; Antipin, M. Y.; Knyazev, S. P.; Kirin, V. N.; Alexeev, N. V.; Chernyshev, E. A. *Mendeleev Commun.* **2000**, 88.

(13) Haaland, A. *Angew. Chem., Int. Ed. Engl.* **1989**, *28*, 992.

(14) Shen, Q.; Hilderbrandt, R. L. *J. Mol. Struct.* **1980**, *64*, 257.

(15) Thorne, L. R.; Suenram, R. D.; Lovac, F. J. *J. Chem. Phys.* **1983**, *78*, 167.

(16) Leopold, K. R.; Canagaratna, M.; Philips, J. A. *Acc. Chem. Res.* **1997**, *30* (2), 57–64.

(17) Vijay, A.; Sathyanarayana D. N. *Chem. Phys.* **1995**, *198*, 345–352.

(18) Binkley, J. S.; Thorne, L. S. *J. Chem. Phys.* **1983**, *79*, 2932.

(19) Shishkov, F.; Khristenko, L. V.; Rudakov, F. M.; Vilkov, L. V.; Karlov, S. S.; Zaitseva, G. S.; Samdal, S. *J. Mol. Struct.*, in press.

(20) Vijay, A.; Sathyanarayana, D. N. *J. Mol. Struct.* **1996**, *375*, 127–141.

(21) Schmid, R.; Boese, R.; Blaser, D. *Z. Naturforsch., B* **1982**, *37*, 1230.

(22) Cambridge Structural Database, Release Oct 2000.

one exception is compound **7**, where the D_N value is significantly larger (0.47 Å), which may be caused by deformation of the atrane cage due to presence of relatively large sulfur atoms.

The M atom usually keeps its expected distorted trigonal-bipyramidal configuration, but the range of its deviation from the plane of equatorial atoms Y (D_M) is varying in a larger interval (0.03–0.4 Å²²). The difference in D_M between the crystal phase and the isolated molecule in 1-methylsilatrane is more pronounced than that in boratrane (the values of D_M are equal to 0.20 and 0.39 Å), which allows one to suggest that variation of the strength of the dative bond in the former compound is stronger.

As far as molecules **1** and **2** in crystals do not form specific intermolecular interactions with exception of a number of rather weak C–H···O hydrogen bonds (distances H···O 2.40–2.57, C···O 3.26–3.57 Å, angles C–H···O 126–159°), we may suggest that the shortening of the B–N and Si···N distances in crystals is caused mainly by the intermolecular dipole–dipole interactions. If it is really the case that geometry of the boratrane molecule in polar media (i.e. in solution) is similar to that in the crystal, the shortening of the B–N bond in such media should be observed as it occurs in BH₃NH₃, where this bond becomes equal to 1.57 Å in the presence of water.²³

Our calculations of the boratrane molecule in water media (details are referred to the Experimental Section) resulted in shortening of the B–N bond up to 1.688 Å in comparison to the isolated molecule (1.8283 and 1.8384 Å for B3LYP/cc-pVDZ and B3LYP/6-311+G(d) calculations). The value obtained is close to the B–N bond length in the crystal. So, the character of the given bond in solution is closer to that in the crystal.

The lengths of the equatorial B–Y bonds in boratrane derivatives **6–8** are close to those for acyclic compounds. This may indicate that there is no significant influence of the atrane cage upon these bonds. On the contrary, the transannular interaction in atranes³ and the length of the B–N bond²⁴ depend significantly on the nature of the equatorial atom Y. In particular, in the series of compounds investigated the largest B–N bond length is observed in the case of equatorial B–O bonds. The length of the B–N bond in the case of B(OH)₃NH₃ is approximately 0.15 Å larger than that in BH₃NH₃, and it is close to the corresponding value in the isolated boratrane.

It is interesting to analyze behavior of the B–N bond in boratrane derivatives **6–8**. The replacement of the oxygen atoms by nitrogen (**6**), sulfur (**7**), or carbon (**8**) does not result in weakening of the B–N bond but in strengthening. Thus, the B–N bond length in the case of Y = NH₂ is equal to 1.696 and 1.699 Å in accord with B3LYP/cc-pVDZ and B3LYP/6-311+G(d) calculations. The observed strengthening of the B–N bond is typical for 2,8,9-triaza derivatives of atranes. For instance, the Si···N distance in 1-phenyl-

2,8,9-triazasilatrane²⁵ (2.132(4) Å) is slightly shorter than that in the α - and β -forms of 1-phenylsilatrane (2.193(5) and 2.156(4) Å)²⁶ and the Si···N bond length in 1-(oxyethyl)-2,8,9-triazasilatrane is also decreased in comparison to that in 1-(oxyethyl)silatrane (2.133 and 2.139 Å, respectively).^{27,28}

The length of the B–N bond in **8** (Y = CH₂, 1.758 Å) is shorter than that in boratrane. On the contrary, in carbon derivatives of silatranes, dative bonds are always elongated in comparison to the parent compound. For instance, the Si···N bond length in crystalline 1-phenyl-2,8-dioxo-5-aza-1-silatricyclo[3.3.3.0]undecane (2.291 Å)²⁹ is longer than in both forms of 1-phenylsilatrane (2.193(5) and 2.156(4) Å).²⁶ Quantum calculations give rise to similar results.³

Analysis of the molecular geometry in isolated and solid states has shown that the strength of the dative B–N bond in boratrane is lower than that for noncyclic donor–acceptor complexes of boron. The strength of the dative bond is affected by both (except for the inductive effect of the X atom) the nature of the equatorial atom Y (in the condensed state), and by the presence of dipole–dipole interactions.

The B–N bond in boratrane and Si···N in 1-methylsilatrane are easily polarized, which allows one to suggest their significant noncovalent nature. Therefore, the peculiarities of the molecular geometry in **1** and **2** coincide with those for acyclic donor–acceptor complexes. To sum up analysis of the molecular geometry, we can suggest that the character of the B–N and Si···N interatomic interactions appears to be similar for dative bonds in acyclic boron complexes¹⁰ and would correspond rather to interactions of the intermediate type.

Topological Analysis of the Electron Density Distribution. Analysis of the experimental electron density distribution has demonstrated considerable difference in the bonding character evidenced from the deformation electron density (DED) maps for **1** and **2**. It can be seen from Figure 4 (left) that in the region of the B–N bond for the compound **1** a continuous concentration of the positive DED is observed that is similar to the pattern found earlier in the crystal of NH₃–BF₃.³⁰ The DED maximum at this bond is equal to 0.40 e Å⁻³, and it is localized at 0.42 Å from the nitrogen atom. The character of the DED in the B–N bond most probably corresponds to the nitrogen Lp's donation to the vacant orbital of the boron atom. The DED maximum (0.45 e Å⁻³) in the region of the Si···N bond is localized at the same distance from the nitrogen atom as in boratrane (0.42 Å). However, in this case the maximum has definitely sharp rather than diffuse character and it is localized mostly at the nitrogen atom rather than between the N and Si atoms (Figure 4, right).

To obtain more information about the electronic structure of the molecules studied, analysis of the $\rho(r)$ function in

(23) Buhl, M.; Steinke, T.; Schleyer, P. v. R.; Boese, R. *Angew. Chem., Int. Ed. Engl.* **1989**, *28*, 992.

(24) Anane, H.; Jarid, A.; Boutalib, A.; Nebot-Gil, I.; Tomas, F. *J. Mol. Struct. (THEOCHEM)* **1998**, *455*, 51–57.

(25) Macharashvili, A. A.; Shklover, V. E.; Struchkov, Y. T.; Lapsina, A.; Zelcans, G.; Lukevics, E. *J. Organomet. Chem.* **1988**, *349*, 23–27.

(26) Parkanyi, L.; Simon, K.; Nagy, J. *Acta Crystallogr. B* **1974**, *30*, 2328.

(27) Gudat, D.; Verkade, J. G. *Organometallics* **1989**, *8*, 2772.

(28) Garant, R. J.; Daniels, L. M.; Das, S. K.; Janakiraman, M. N.; Jacobson, R. A.; Verkade, J. G. *J. Am. Chem. Soc.* **1991**, *113*, 5728.

(29) Hencsei, P.; Kovacs, I.; Parkanyi, L. *J. Organomet. Chem.* **1985**, *293*, 185.

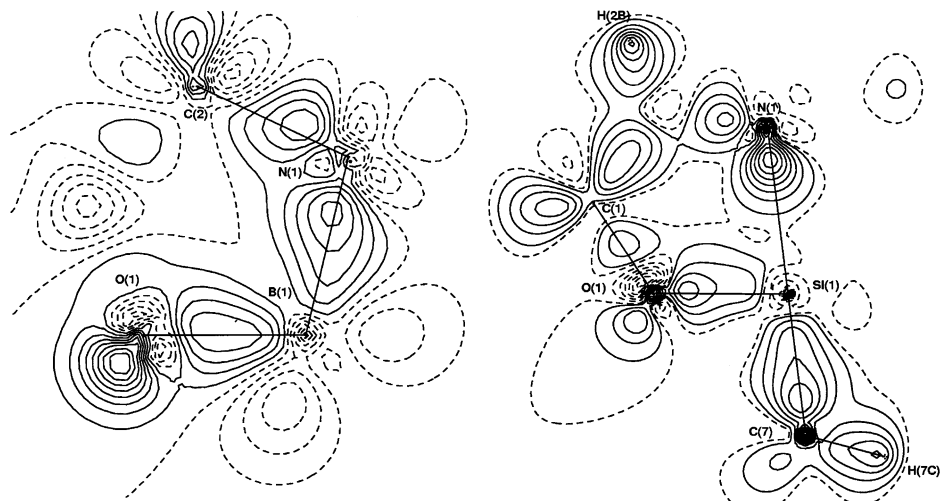


Figure 4. Multipole static DED maps for the compounds **1** (left) and **2** (right) in the N–M–O planes. Isolines are drawn through $0.1 \text{ e}/\text{Å}^3$, and negative contours are dashed.

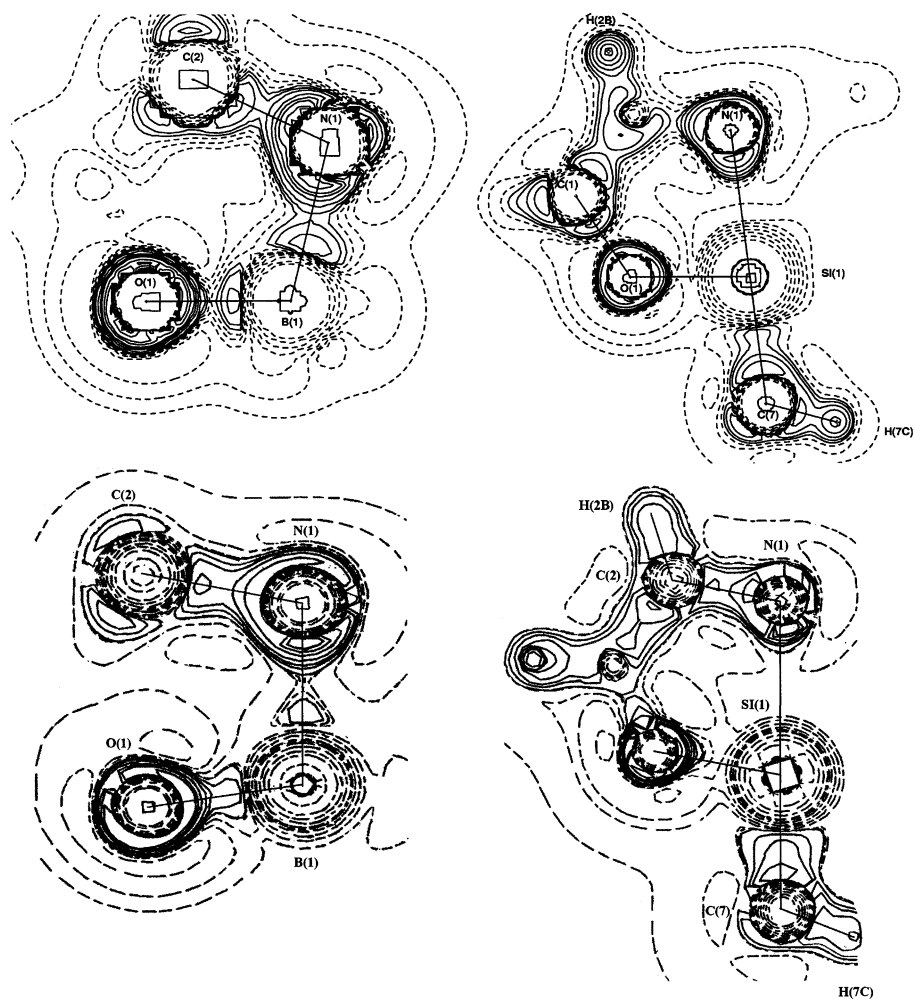


Figure 5. Maps of the negative Laplacian $-\nabla^2\rho(r)$ in the logarithmic scale for the compounds **1** (left) and **2** (right) in the planes N–M–O. Values of $\nabla^2\rho(r) > 0$ are dashed. Theoretical maps are given below the experimental ones.

terms of the AIM theory has been done. Both the experimental and theoretical $-\nabla^2\rho(r)$ maps (Figure 5) are in accord with DED sections and indicate that the $\rho(r)$ concentration is observed in all expected bonds including regions of the B–N and Si \cdots N interactions. Analysis of the DED and $-\nabla^2\rho(r)$ maps has demonstrated also that donation of the

Lp of the nitrogen atom in boratrane is considerably stronger than that in 1-methylsilatrane.

The CP's(3,–1) are located at all chemical bonds including the B–N and Si \cdots N lines. Topological characteristics of the bonds, namely values of the $\nabla^2\rho(r)$, $\rho(r)$, and $E(r)$ in CP-(3,–1) are summarized in Table 2.

Table 2. Topological Characteristics of the Electron Density Distribution in **1–8**

method	1		2		3	4	5		6		7		8	
	B–N	B–O	Si···N	Si–O	B–N	B–N	B–N	B–O	B–N	B–N	B–N	B–S	B–N	B–C
	$\rho(r)$ in CP(3,–1) (e/au ³)													
expt	0.14	0.18	0.07	0.15										
B3LYP/6-311+G(d)	0.09	0.17	0.04	0.12	0.19	0.10	0.09	0.18	0.11	0.17	0.11	0.13		
B3LYP/cc-pVDZ	0.09		0.04	0.12	0.19	0.10	0.13	0.14	0.11	0.16	0.11	0.13	0.09	0.16
	$\nabla\rho(r)$ in CP(3,–1) (e/au ⁵)													
expt	–0.2	0.21	0.04	0.10										
B3LYP/6-311+G(d)	–0.006	0.61	0.26	0.09	0.39	0.41	0.43	0.60	0.23	0.18	0.12	–0.25		
B3LYP/cc-pVDZ	–0.02	0.84	0.28	0.09	0.73	0.48	0.49	0.49	0.24	0.39	0.12	–0.25	0.21	–0.51
	$E(r)$ in CP(3,–1) (H/au ³)													
expt	–0.13	–0.16	–0.03	–0.09										
B3LYP/6-311+G(d)	–0.07	–0.15	–0.01	–0.21	–0.18	–0.05	–0.08	–0.14	–0.08	–0.15	–0.08	–0.11		
B3LYP/cc-pVDZ	–0.07	–0.11	–0.03	–0.20	–0.14	–0.06	–0.06	–0.10	–0.08	–0.13	–0.08	–0.12	–0.06	–0.31

A clear distinction between the closed-shell or intermediate type of interatomic interaction is impossible without determination of the local energy density, which is directly retrieved from calculations but cannot to be obtained experimentally (the $E(r)$ value may be evaluated empirically from the $\nabla^2\rho(r)$ and $\rho(r)$ values according to ref 31).

The presence of the intramolecular B–N and Si···N interactions in **1** and **2** must result in formation of three CP-(3,+1), thereby indicating formation of the corresponding five-member cycles. These CP's were also detected in topological analysis of $\rho(r)$ in the compounds studied.

Experimental topological characteristics of the chemical bonds (Table 2) are close to theoretical ones and to the data for MP2 calculation of BH_3NH_3 .^{10,18} The similarity of these characteristics of $\rho(r)$ demonstrates that our selected theoretical level (B3LYP/6-311+G(d) and B3LYP/cc-pVDZ) may be successfully used for analysis of bonding patterns in the compounds of interest in terms of their $\rho(r)$ topology.

The bonds in the atrane framework of **1** and **2** (except the Si–O and B–O bonds) are characterized by negative values of both the $\nabla^2\rho(r)$ and $E(r)$ in the CP(3,–1). So, these bonds may be described as shared (covalent) interactions. The values of $\nabla^2\rho(r)$ are in agreement with corresponding data usually observed in crystals of organic compounds.^{32–34} On the contrary, at the CP(3,–1) of the B–O and Si–O bonds, positive values of $\nabla^2\rho(r)$ are observed. However, the values of $E(r)$ for these bonds, both in the crystal and isolated molecules, still have a negative sign and the magnitudes of $\rho(r)$ at CP's(3,–1) are large enough. Thus, according to the AIM theory, equatorial B–O and Si–O bonds in **1** and **2** are classified as intermediate types of interatomic interactions. This is consistent with the results of a number of earlier experimental and theoretical investigations.^{35a–d} Such a character of the Si–O and B–O bonds is probably caused by their high polarity and by a repulsion between bonding

Table 3. Topological Properties of the Boron Atom

compd	method/basis	r_{BN} (Å)	r_{BY} (Å)	$r_{\text{S}}(\text{BN})$	$r_{\text{S}}(\text{BY})$
1	B3LYP/6-311+G(d)	0.632	0.465	0.93	0.89
	B3LYP/cc-pVDZ	0.627	0.471	0.94	0.90
	X-ray	0.574	0.483	0.93	0.91
6	B3LYP/6-311+G(d)	0.527	0.494	0.86	0.88
	B3LYP/cc-pVDZ	0.531	0.501	0.86	0.89
7	B3LYP/6-311+G(d)	0.544	0.603	0.86	0.87
	B3LYP/cc-pVDZ	0.546	0.617	0.87	0.88
8	B3LYP/cc-pVDZ	0.547	0.512	0.86	0.86

electron density and the Lp's of oxygen atoms (lone-pair weakening effect).³⁶ Topological parameters of the electron density for B–O bonds in isolated molecules for boratrane and $(\text{OH})_3\text{BNH}_3$ are identical. This allows one to conclude that the influence of the atrane cage on the B–O bond is negligible.

Analysis of the topological parameters of the B–N bonds in noncyclic compounds BH_3NH_3 and $(\text{OH})_3\text{BNH}_3$ has revealed positive values of $\nabla^2\rho(r)$ and negative ones for $E(r)$. So, B–N bonds in **4** and **5** are also referred to interactions of an intermediate type. On the other hand, the theoretical calculation of $\text{B}(\text{NH}_2)_3$ has revealed that the same intermediate type of interaction is observed for an a priori single covalent B–N bond which remains unchanged upon transition from the gas to the crystalline state. Probably, the intermediate type of interaction is a general feature of a quite labile B–N bond.

We suggested earlier the close similarity between the B–N and Si···N bonds basing only on the molecular geometry parameters. However, results of the qualitative analysis of the $\rho(r)$ distributions (Figures 4 and 5) contradict this assumption. Below, the bonding pattern in **1** and **2** will be discussed in detail.

Analysis of the $\rho(r)$ topology in 1-methylsilatrane (**2**) has revealed the that Si···N bond is characterized by a positive value of $\nabla^2\rho(r)$ and a negative one for $E(r)$ in CP(3,–1). Thus, similarly to the B–N bonds in acyclic complexes **4**

(30) Antipin, M. Y.; Slovokhotov, Y. L.; Yanovsky, A. I.; Struchkov, Y. T. *Dokl. Acad. Nauk USSR* **1985**, *281*, 340.

(31) Abramov, Y. A. *Acta Crystallogr.* **1997**, *A53*, 264.

(32) Roversi, P.; Barzaghi, M.; Merati, F.; Destro, R. *Can. J. Chem.* **1996**, *74*, 1145.

(33) Koritsanszky, T.; Buschmann, J.; Luger, P. *J. Phys. Chem.* **1996**, *100*, 10547.

(34) Birger, D.; Flaig, R.; Koritsanszky, T.; Krane, H.; Morgenroth, W.; Luger, P. *Chem.—Eur. J.* **2000**, *6* (14), 2582.

(35) (a) Gibbs, G. V.; Boisen, M. B.; Hill, F. C.; Tamada, O.; Downs, R. T. *Phys. Chem. Mater.* **1998**, *25*, 574. (b) Hill, F. C.; Gibbs, G. V.; Boisen, M. B., Jr. *Phys. Chem. Mater.* **1997**, *24*, 582. (c) Downs, J. W.; Swope, R. J. *J. Am. Chem. Soc.* **1992**, *96*, 4830. (d) Kuntzinger, S.; Dahaoui, S.; Ghermani, N. E.; Lecomte, C.; Howard, J. A. K. *Acta Crystallogr., Sect. B* **1999**, *55*, 867.

(36) Snaik, S.; Maitre, P.; Sini, G.; Hiberty, P. C. *J. Am. Chem. Soc.* **1992**, *114*, 7861.

Table 4. Crystal Data for **1** and **2**

	1	2
mol formula	BO ₃ C ₆ H ₁₂	SiO ₃ C ₇ H ₁₅
fw	156.98	189.29
color, shape	colorless, prism	colorless, prism
dimens (mm)	0.3 × 0.2 × 0.2	0.4 × 0.3 × 0.2
cryst system	orthorhombic	monoclinic
space group	<i>Pna</i> 2 ₁	<i>P2</i> ₁ / <i>c</i>
<i>a</i> (Å)	11.300(2)	7.5663(1)
<i>b</i> (Å)	6.554(1)	12.0408(2)
<i>c</i> (Å)	9.618(2)	9.6210(1)
β (deg)		91.740(1)
<i>V</i> (Å ³)	712.4(2)	876.11(2)
<i>Z</i>	4	4
ρ_{calc} (g cm ⁻³)	1.464	1.435
temp (K)		100
scan type	ω (0.3° step in ω and 10 s exposure for θ range 2.533.5° and 25 s for θ range 33.557.5°)	ω (0.3 step in ω and 20 s exposure/frame)
$\sin(\theta/\lambda)$ (Å ⁻¹)	1.187	1.000
radiation, λ (Mo K α) (Å)	0.710 72	
linear abs (μ) (mm ⁻¹)	0.112	0.236
abs corr		SADABS
<i>T</i> _{min} / <i>T</i> _{max}	0.98/0.82	0.96/0.79
<i>F</i> (000)	336	408
tot. reflcns (<i>R</i> _{int})	26724 (0.0402)	20349 (0.0135)
no. of indepndt reflcns	7359	7397
no. of indepndt reflcns with <i>I</i> > 2(σ)	6070	6305
params	148	169
wR ₂	0.0966	0.0911
R ₁ (multipole refinement)	0.0410 (0.0247)	0.0307 (0.0211)
GOF (multipole refinement)	0.971 (1.499)	1.031 (1.69)
$\rho_{\text{max}}/\rho_{\text{min}}$ (e Å ⁻³)	0.666/0.284	1.101/0.283

and **5**, we can consider the Si···N bond in this compound as an interaction of the intermediate type.

Surprisingly, in contrast to **2–5**, in boratrane both in the crystal (−0.20 ae) and in the isolated molecule (−0.02 and −0.006 ae for B3LYP/cc-pVDZ and 6-311+G(d) calculations, respectively) the observed value of the $\nabla^2\rho(r)$ is negative. The theoretical value of $\nabla^2\rho(r)$ depends on choice of the basis set, but certainly the constancy of the sign of the Laplacian is kept. Additionally, an excellent agreement between the predicted and experimental (ED) geometry gives us strong support that topological parameters of the B–N bond in **1** are not an artifact of calculations. In turn, the difference between experimental and theoretical values of $\nabla^2\rho(r)$ in CP(3,−1) is consistent with elongation of the B–N bond in the gas phase.

Topological parameters of the B–N bond (experimental and theoretical ones) in **1** correspond not to interaction of the intermediate type as it appears in the case of acyclic compounds BH₃NH₃ and (OH)₃BNH₃ but to the shared interaction. It is noteworthy that the experimental value of $\rho(r)$ in CP(3,−1) for the B–N bond is much larger than corresponding values in model acyclic compounds **4** and **5**, where such a bond is formed by a donor–acceptor mechanism and it is comparable with that in B(NH₂)₃. The differences in topological parameters of the B–N bond between **1** and **3–5** appear more intriguing taking into account significant polarizability of the B–N bond in boratrane and its greatest shortening upon transition from the crystal to isolated molecule (0.15 Å).

Previous theoretical investigation of the series of donor–acceptor boron complexes¹⁰ has revealed that the local energy density correlates with ab initio calculated energy of the B–N

bond. Therefore it is useful to compare the $E(r)$ values for the B–N bond in boratrane **1** and in the model compounds **3** and **4**.

The experimental value of $E(r)$ in CP(3,−1) estimated empirically³¹ for the B–N bond in boratrane (−0.13 ae) is close to that in B(NH₂)₃, where this bond is covalent in terms of the “classical” Lewis model³⁷ (see Table 2). Besides, this $E(r)$ value is much higher than that for acyclic compounds **4** and **5**. So, if the correlation between $E(r)$ and energy of the B–N bond is valid for atrane compounds, the B–N bond in the crystal of boratrane is comparable to that in B(NH₂)₃. Taking into account that the B–N bond corresponds to the intermediate type of interaction for both compounds **3** and **5**, it becomes more evident that unusual topology of $\rho(r)$ in boratrane (**1**) may be dictated by the presence of the atrane cage.

Thus, one can expect that B–N bonds in boratrane derivatives **6–8** as well as in boratrane itself have the same type of shared interatomic interactions. The characteristic set of CP's in **6–8** is similar to that in **1** including the presence of CP(3,−1) in the interatomic B–N region. Topological parameters of the CP's(3,−1) for C–C and C–N bonds of the atrane cage are identical to those in boratrane. Nevertheless, despite the considerably shortened B–N bond length, an interaction of intermediate type is observed in all cases (**6–8**). It should be noted that $E(r)$ values in all boratrane derivatives are similar. Consequently, apart from steric restraints, electronic effects play a significant role in boratrane structure. One may assume that the

(37) Lewis, G. N. *Valence and Structure of Atoms and Molecules*; The Chemical Catalog Co. Inc.: New York, 1923.

sum of the steric and electronic effects leads to changing of the volume and shape of the boron atom, which was examined in terms of AIM theory, namely in terms of the atom's volume (V_{at}) and bond radii r — the distance from the nuclei to CP(3,−1).

Our estimation of the V_{at} value as the 0.002 ae envelope of $\rho(r)$ in the boratrane molecule and its derivatives has demonstrated that the volume of the boron atom remains unchanged (0.52 au³) and no dependence on the nature of the equatorial atom Y is observed. Taking into account that the bond radii depend on differences of electronegativities of the bonded atoms, we can expect that a similar analysis could help to evaluate variations of the shape of the boron atom in compounds **1** and **6–8**.

To account for the differences in the B–N bonds, in this work we used empirically reduced bond radii r_s scaled to the bond length as $r_s = [\ln(l_{B-N} \text{ (or B-Y)}/r)]^{-1}r$, where l_{B-N} corresponds the B–N bond length and r corresponds the bond radius of the B–N bond r_{BN} or B–Y bond r_{BY} . The values of $r_s(BN)$ for compounds **6–8** remained almost unchanged (~ 0.86 , Table 3). Also, changing the nature of the equatorial atoms does not influence the values of the reduced bond radii $r_s(BY)$. Thus, analysis the values of the reduced bond radii allows one to conclude that boron atom shape in **6–8** remains unchanged for Y = N, S, and C.

Despite the similarity of the $r_s(BY)$ values, the B–Y bonds in **6–8** are characterized by a different type of interatomic interaction. In particular, the B–S and B–C bonds correspond to shared interactions, while the B–N bond in **6** corresponds to an interaction of the intermediate type. Consequently, the character of the transannular B–N interaction in **6–8** almost does not depend on the polarity of the B–Y bond, i.e., electronegativity of equatorial atoms.

The main difference from the model compounds **6–8** is observed for **1** where the value of $r_s(BN)$ is much larger (0.93 and 0.94 for B3LYP/6-311+G(d) and B3LYP/cc-pVDZ calculations; see Table 3). However, corresponding values for equatorial bonds $r_s(BY)$ are close to those for **6–8**. Thus, the influence of the oxygen atoms results in distortion of the shape of the boron atom and leads to displacement of CP(3,−1) of the B–N bond toward concentration of $\rho(r)$ at Lp of the nitrogen atom. Such a “pushing” of the boron atom within the atrane cage changes the character of the B–N bond in boratrane to opposite direction in comparison to model compounds **6–8** and **2**. Taking into account that the B–O bond has the shortest length among all B–Y bonds and highest concentration of the electron density around the oxygen atoms that are not directly involved in chemical bonding, one may conclude that the “electronic part” of the atrane cage effect may be related to the pushing of the boron atom into the cage by means of oxygen Lp's.

Conclusion

X-ray diffraction analysis and theoretical calculations have demonstrated that the atrane cage effect is a sum of different factors, namely a steric influence of the atrane cage and electronic influence of the oxygen atoms. This effect can

account for high hydrolytic stability of the boratrane as well as silatranes and germatranes. A direct comparison of only the transannular interaction in silatranes and boratranes may be considered in terms of the different extents of the atrane cage effect in these compounds. It should be kept in mind, however, that the electron configurations of silicone and boron atoms are different, and in particular for boratrane, the effect of the atrane cage is more pronounced due to the shortest equatorial and dative bonds lengths. In silatranes and germatranes the cage effect probably also plays a significant role since the hydrolytic stability of a number of silatranes and germatranes is well-known, while acyclic compounds of silicon, like Si(OC₂H₅)₄, rapidly decompose in the presence of water.¹

Experimental Section and Calculation Details

All X-ray diffraction measurements were carried out with a SMART 1000 CCD diffractometer at 100 K and monitored by the SMART program.³⁸ The frames were integrated and corrected by SAINT and SADABS programs.^{38,39} Details of crystallographic data and experimental conditions are presented in Table 4. Important structural parameters of structures **1** and **2** are summarized in Table 1.

The structures were solved by direct methods and refined by the full-matrix least-squares technique against F^2 in the anisotropic–isotropic approximation. Hydrogen atoms were located from the Fourier synthesis and refined in the isotropic approximation. All calculations were performed using SHELXTL 97⁴⁰ on an IBM PC/AT.

The analytical form of the experimental electron density was obtained by a multipole refinement based on the Hansen–Coppens⁴¹ formalism using the XD program package.⁴² The level of the multipole expansion was hexadecapole for the Si(1) and N(1) atoms, octadecapole for all oxygen, carbon, and boron atoms, and dipole for hydrogens. The scattering factor of the hydrogen atoms was calculated from the contracted radial density functions ($\kappa = 1.2$). The ratio of the number of reflections to the number of refined parameters was more than 20. Quantum calculations were carried out using the B3LYP/6-311+G(d) and B3LYP/cc-pVDZ method/basis by means of Gaussian98W⁴³ program. To analyze electron

- (38) Programs SMART 1998 and SAINT 1999, Bruker-AXS Inc., Madison, WI.
- (39) Sheldrick, G. M. *SADABS*, v.2.01; Bruker/Siemens Area Detector Absorption Correction Program; Bruker AXS: Madison, WI.
- (40) Sheldrick, G. M. *SHELXTL-97*, V5.10; Bruker AXS Inc.: Madison, WI 53719, 1997.
- (41) Hansen, N. K.; Coppens, P. *Acta Crystallogr.* **1978**, A34, 909–921.
- (42) Koritsansky, T.; Howard, S. T.; Richter, T.; Mallinson, P. R.; Su, Z.; Hansen, N. K. XD, a computer program package for multipole refinement and analysis of charge densities from X-ray diffraction data, 1995.
- (43) Frisch, M. J.; Trucks, G. W.; Schlegel, H. B.; Scuseria, G. E.; Robb, M. A.; Cheeseman, J. R.; Zakrzewski, V. G.; Montgomery, J. A.; Stratmann, R. E.; Burant, J. C.; Dapprich, S.; Millam, J. M.; Daniels, A. D.; Kudin, K. N.; Strain, M. C.; Farkas, O.; Tomasi, J.; Barone, V.; Cossi, M.; Cammi, R.; Mennucci, B.; Pomelli, C.; Adamo, C.; Clifford, S.; Ochterski, J.; Petersson, G. A.; Ayala, P. Y.; Cui, Q.; Morokuma, K.; Malick, D. K.; Rabuck, A. D.; Raghavachari, K.; Foresman, J. B.; Cioslowski, J.; Ortiz, J. V.; Stefanov, B. B.; Liu, G.; Liashenko, A.; Piskorz, P.; Komaromi, I.; Gomperts, R.; Martin, R. L.; Fox, D. J.; Keith, T.; Al-Laham, M. A.; Peng, C. Y.; Nanayakkara, A.; Gonzalez, C.; Challacombe, M.; Gill, P. M. W.; Johnson, B.; Chen, W.; Wong, M. W.; Andres, J. L.; Gonzalez, C.; Head-Gordon, M.; Replogle, E. S.; Pople, J. A. *GAUSSIAN 98*, revision A7; Gaussian, Inc.: Pittsburgh, PA, 1998.

Boratrane and 1-Methylsilatrane

density distribution the AIMPAC program package⁴⁴ was used. Solution effects were applied using the polarizable dielectric model.⁴⁵ Molecular geometry and topological characteristics of the compounds studied are presented in Tables 1 and 2.

(44) Cheeseman, J.; Keith, T. A.; Bader, R. W. F. *AIMPAC program package*; McMaster University: Hamilton, Ontario, Canada, 1992.

(45) Miertus, S.; Scrocco, E.; Tomasi, J. *Chem. Phys.* **1981**, *55*, 171.

Acknowledgment. This work was supported by the Russian Foundation for Basis Research, Grant Nos. 00-15-97359, 00-03-32807a, and 99-07-90133.

Supporting Information Available: X-ray data in the form of CIF files. This material is available free of charge via the Internet at <http://pubs.acs.org>.

IC010842E